HHS Public Access

Author manuscript

Int Forum Allergy Rhinol. Author manuscript; available in PMC 2019 December 01.

Published in final edited form as:

Int Forum Allergy Rhinol. 2018 December ; 8(12): 1412–1420. doi:10.1002/alr.22199.

Nasal Polyp Fibroblasts Modulate Epithelial Characteristics Via Wnt Signaling

Alex Dobzanski, MS[1], **Syed Muaz Khalil, PhD**[1], and **Andrew P. Lane, MD**[1]

[1]Department of Otolaryngology-Head and Neck Surgery, Johns Hopkins University School of Medicine, Baltimore, MD

Abstract

Introduction—While essential to the normal differentiation of ciliated airway epithelial cells, upregulated Wnt signaling in chronic rhinosinusitis with nasal polyps (CRSwNP) has been proposed to result in abnormal epithelial morphology and dysfunctional mucociliary clearance. The mechanism of epithelial Wnt signaling dysregulation in CRSwNP is unknown, and importantly cellular sources of Wnt ligands in CRSwNP have not yet been investigated.

Methods—Human sinonasal epithelial cells (hSNECs) and fibroblasts (hSNFs) were collected from thirty-four human subjects (25 control and 9 CRSwNP) and differentiated as primary ALI and organoid co-cultures. hSNECs were isolated to the apical compartment of the transwell and hSNFs were isolated to the basolateral compartment. After 21 days of ALI culture, ciliary expression and sinonasal epithelial morphology were examined by immunohistochemistry (IHC) and quantitative real-time polymerase chain reaction (qRT-PCR). An organoid model was used to evaluate proliferation of basal cells in presence of hSNFs.

Results—Epithelial cells co-cultured with CRSwNP-hSNFs revealed significantly decreased ciliated cells, altered epithelial cell morphology, and increased colony forming efficiency compared to epithelial cells co-cultured with control-hSNFs. CRSwNP-hSNFs showed significantly higher mRNA expression of canonical *WNT3A*. A Wnt agonist, CHIR99021, replicated CRSwNP-hSNF co-cultures, and treatment with the Wnt inhibitor IWP2 prevented abnormal morphologies.

Discussion—These results suggest that abnormal interactions between epithelial cells and fibroblasts may contribute to CRSwNP pathogenesis and supports the concept that dysregulated Wnt signaling contributes impairment to epithelial function in CRSwNP.

Keywords

ciliation; barrier; chronic rhinosinusitis with nasal polyps; Wnt; organoid; epithelial-mesenchymal transition

Corresponding Author: Andrew Lane, MD, Department of Otolaryngology- Head and Neck Surgery, Johns Hopkins Outpatient Center, 6th Floor, 601 N. Caroline Street, Baltimore, MD 21287, alane3@jhmi.edu.

Disclosures: Authors declare no relevant or material financial interests that relate to the research described in this paper.

Presented at the ARS COSM meeting on April 19–20, 2018

Introduction

Chronic rhinosinusitis with nasal polyps (CRSwNP) is a subgroup of chronic rhinosinusitis (CRS) with a prevalence of up to 4% of the US population [1–3]. While only 25–30% of patients with CRS have nasal polyps, the disease is associated with rhinorrhea, nasal congestion, hyposmia and facial pressure resulting in a significant decrease in quality of life [1]. Nasal polyposis is challenging to manage and is frequently recalcitrant to medical and surgical therapy [1–5]. The pathogenesis of CRSwNP remains unclear, but the condition is characterized physiologically by inflammation and epithelial remodeling involving barrier disruption and decreased mucociliary clearance (MCC) [5]. MCC is an integral component of innate immunity, providing a first line of defense against aerosolized pathogens and debris [4, 6]. Epithelial goblet cells secrete mucus that is then propelled by the coordinated ciliary beating of multiciliated cells. Disrupted organization of the epithelium and insufficient ciliated cells impair MCC leading to defective innate barrier function [7, 8].

While essential to the normal differentiation of ciliated airway epithelial cells, upregulated Wnt signaling in CRSwNP has been proposed to result in abnormal epithelial cell morphology and dysfunctional MCC [8–10]. In the lung, Wnt derives from epithelial and subepithelial mesenchymal cell populations, including fibroblasts [8, 9, 11, 12]. Wnt ligands are known to regulate proliferation, differentiation, adhesion, migration, and stem cell self-renewal through activation of the Wnt/β-catenin canonical pathway, non-canonical planar cell polarity pathway, or Wnt/Ca^{2+} pathway [13]. Non-canonical Wnt signaling is important for alignment of cilia and effective MCC. Interestingly, it is the canonical Wnt pathway that has been shown to increase in both the epithelium and submucosa in nasal polyps, although the cellular sources of Wnt ligand expression in nasal polyps have not been identified [8].

Proper airway development requires complex expression and timing of Wnt that is upregulated during proliferation and decreases once differentiated [9, 14, 15]. Canonical Wnt ligands, such as the prototypical canonical ligand Wnt3a, activates frizzled receptors on Wnt responsive cells, leading to inhibition of β-catenin degradation. Accumulation of β-catenin in the cytosol localizes to the nucleus and complexes with transcription factors lymphoid enhancing factor/T cell factor (Lef/Tcf) to regulate target gene expression. β-catenin from the cytosol can also be stabilized by E-cadherin expressed in epithelial adherins junctions [8, 9]. The presence of Wnt, loss of E-cadherin, and increased β-catenin are defining characteristics of epithelial-mesenchymal transition (EMT) [13]. The mechanism of Wnt signaling dysregulation in CRSwNP remains unelucidated.

Here, we use a co-culture model of epithelial cells with control- or CRSwNP-hSNFs to evaluate ciliation, morphology, permeability and proliferation of epithelial cells. Furthermore, we propose a mechanism involving hSNF-derived Wnt signaling that may underlie the dysregulated epithelium in CRSwNP.

Methods

Human subjects

Thirty-four adult subjects undergoing endonasal surgical procedures were enrolled in this study to allow collection of epithelial and/or fibroblasts from brushings (CytoSoft Cytology Brush, Medical Packaging Corperation, Camarillo, CA) or from discarded sinonasal surgical tissue. Twenty-five control subjects without CRS were undergoing endonasal approaches for treatment of skull base or orbital pathology. Nine subjects had CRSwNP defined by the presence of diffuse sinonasal polyposis on endoscopy, with tissue eosinophilia by histology. Patients with cystic fibrosis or primary ciliopathies were excluded from the study. The research protocol was approved by the Institutional Review Board and all subjects gave signed informed consent.

Air-liquid interface cell culture

Control hSNECs used for primary culture were obtained by sinonasal brushing of patients undergoing sinus surgery [16]. Epithelial cells were seeded onto collagen-IV-coated (Sigma-Aldrich, St. Louis, MO) transwell plates (Corning, Corning, NY) and expanded to confluence in expansion media (Pneumacult-Ex Plus, Stemcell Technologies, Vancouver, Canada). After confluent, the apical media was aspirated and the basolateral media was replaced with ALI media (Pneumacult-ALI, Stemcell Technologies, Vancouver, Canada). The cells were considered fully differentiated after 21 days of ALI.

For epithelial-fibroblast combined-culture model, collagen-IV coated transwell inserts were removed from the transwell plate and stored while either control- or CRSwNP-hSNFs were seeded on the basolateral surface of the plate at a density of 10^4 cells/cm^2. Wells were coated with Fibronectin (Sigma-Aldrich, St. Louis, MO) and hSNFs were grown in fibroblast growth medium (10% FBS, 1% Glutamax, 1% Pen/strep, 1% NEAA in DMEM) until confluent, usually 1–2 days. After confluent, collagen-IV-coated transwell inserts were placed back into the transwell plate and control hSNECs were then seeded on the apical surface in expansion media. Once hSNECs were confluent, apical media was aspirated and basolateral media was replaced with ALI.

To study the effects of canonical Wnt signaling, either 2.5μM IWP2 (StemMACS, Miltenyi Biotech, Bergisch Gladbach, Germany), a Wnt inhibitor, or 3μM CHIR99021 (Tocris Bioscience, Bristol, United Kingdom), a canonical Wnt activator, were added to the basolateral compartment beginning the first day of ALI for 21 days.

hSNEC organoid culture

hSNECs expanded on collagen-I (Sigma-Aldrich, St. Louis, MO) coated 100mm plate (Corning, Corning, NY) were dissociated, centrifuged, resuspended in 1:1 Reduced Growth Factor Matrigel (Corning, Corning, NY) and ALI. Cells were then seeded at a density of 1,000 cells per 24-well transwell, which was precoated with Matrigel. Organoids were fed with Pneumacult-ALI in the basolateral compartment until analysis at day 10. Present in the basolateral compartment were either control- or CRSwNP-hSNFs seeded onto Fibronectin-coated wells, described in cell culture methods. hSNFs were confluent before hSNECs/

Matrigel were seeded on the apical side of the transwell. There was no direct contact between cell types.

Real Time–Quantitative PCR

RNA was extracted using Direct-zol RNA MiniPrep (Zymo Research, Irvine, CA) and was reverse transcribed using Omniscript RT Kit (Qiagen, Hilden, Germany) by following the manufacturer's protocol. Real time–quantitative PCR reactions were performed in StepOnePlus Real-Time PCR System (Applied Biosystems, Foster City, CA) using SYBR Green MasterMix (ThermoFisher, Waltham, MA) and predesigned *18s*, *TUBB4B, FOXJ1, WNT3A, WNT4, WNT5A, and CTNNB1* primers by Invitrogen. Gene expression levels were normalized to *18s*, and relative changes were determined using the $2^{-\Delta\Delta Ct}$ method.

Immunocytochemistry

Adherent hSNECs on transwell membrane were fixed in 4% paraformaldehyde. After permeabilization with 0.5% Triton-X (EMD Chemicals, Gibbstown, NJ) and blocking of nonspecific binding sites with 10% donkey serum, cells were incubated (4°C, overnight) with mouse anti-β-tubulin IV (abcam, Cambridge, United Kingdom), rabbit anti-E-cadherin (Cell Signaling, Danvers, MA), goat anti-FOXJ1 (R&D, Minneapolis, MN). Secondary antibody was applied for 1 hour with Alexa 488-conjugated donkey anti-mouse, Alexa 568-conjugated donkey anti-rabbit, Alexa 633-conjugated donkey anti-goat (Jackson, West Grove, PA). Each sample was counterstained by the nuclear stain, 4′,6-diamidino-2-phenylindole (DAPI) (Vector Labs, Burlingame, CA). The transwell membrane was removed using a scalpel, mounted onto glass slides and visualized using a Zeiss 700 confocal microscope (Carl Zeiss, Jena, Germany). Images were displayed as Z stacks with a 1μm slice thickness starting at the transwell membrane and finishing after cilia were no longer visible. Relative immunofluorescence intensity was calculated by normalizing conditioned values to the mean intensity of untreated hSNECs measured using the Mean Gray Value function of ImageJ software (National Institutes of Health).

Cultured hSNFs were fixed in 4% paraformaldehyde. After permeabilization with 0.1% Triton-X (EMD Chemicals, Gibbstown, NJ) and blocking of nonspecific binding sites with 10% donkey serum, hSNFs were incubated (4°C, overnight) with rabbit anti-Wnt3a (Bioss USA, Woburn, MA), mouse anti-CD90 (Novus Biologicals, Littleton, CO), and goat anti-vimentin (Millipore, Burlington, MA). Secondary antibody was applied for 1 hour with Alexa 488-conjugated donkey anti-mouse, Alexa 568-conjugated donkey anti-rabbit, Alex 633-conjugated donkey anti-goat (Jackson). Each sample was counterstained with DAPI.

In vitro permeability: paracellular fluorescein isothiocyanate-dextran flux

In vitro permeability was evaluated by quantifying paracellular flux of 4-kDa fluorescein isothiocyanate (FITC)–dextran beads [17]. Briefly, 2 mg/mL 4kDa FITC-dextran beads were incubated on the apical surface of hSNEC culture for four hours. After this time, the basolateral medium was collected and read for fluorescence in quadruplicate on a plate reader at an excitation wavelength of 485 nm and an emission wavelength of 528 nm.

Flow cytometry

Cells were washed with PBS and labeled with a live/dead dye (Zombie Aqua, BioLegend) for 15 min at RT and in dark. After centrifugation, the cells were blocked with Fc receptor binding inhibitor monoclonal antibody (Anti-human; eBioscience) in Flow Buffer (PBS + 2% FBS + 2mM EDTA) for 15 min at room temperature. For the detection of fibroblasts, cells were stained with Alexa Fluor 700-conjugated anti-CD90 (BioLegend) and excluded cells positive for APC-Cy7-conjugated anti-CD31 and anti-CD45 (BioLegend). For intracellular cytokine staining, surface-stained cells were fixed in 4% paraformaldehyde (Electron Microscopy Sciences) for 20 min at RT in dark. After two washes, the cells were permeabilized in 0.1% saponin (Sigma) for 10 min at RT in dark. Cells were then stained with Alexa Fluor-488 anti-Wnt3a (R&D). Samples and controls were analyzed on an LSRII flow cytometer (BD Biosciences) using FACSDiVa (BD Biosciences) and FlowJo data analysis software package (TreeStar, USA). Acquired data was gated to include only single cells (FSC-W/FSC-H and SSC-W/SSC-H) that were live (FSC-A/Aqua). Positive cellular expression of markers was gated based on Fluorescence Minus One (FMO) controls.

Statistical analysis

Experiments were performed in triplicate at $n \geq 3$. Results depict mean±SEM. Statistical significance was determined by two-tailed unpaired T test with equal variance. Statistical significance was considered to be $p<0.05$. Results were analyzed with the use of the statistical software Prism 7.3 (GraphPad, La Jolla, CA).

Results

Nasal polyp derived fibroblasts have higher canonical Wnt gene expression

Because Wnt ligands have been reported to play a role in ciliary differentiation, mRNA expression of prototypical Wnt ligands were assessed in control- and CRSwNP-hSNFs [8, 9]. This analysis revealed that CRSwNP-hSNFs had higher gene expression of canonical Wnt ligands, *WNT3A* and *WNT4*, compared to control-hSNFs, however only *WNT3A* was significant (3.62±0.81 vs 1.00±0.40, $p<0.05$) (Figure 1a). While there was a trend towards decreased non-canonical *WNT5A* mRNA expression, this did not reach statistical significance.

Immunofluorescent staining of hSNF cultures with Wnt3a and markers of fibroblasts, CD90 and vimentin, showed an increased percentage of Wnt3a+ fibroblasts from patients with CRSwNP (6.97±0.92 vs 28.18±3.80, $p<0.01$) (Figure 1b, c). To validate the immunofluorescence quantification, we used flow cytometry to assess the percentage of Wnt3a+ fibroblasts from whole tissue of control and CRSwNP patients. Fibroblasts were identified as being positive for fibroblast marker, CD90, and negative for markers of hematopoietic cells and endothelial cells (CD45−CD31−CD90+). From this lineage, we analyzed the percentage that was Wnt3a+ (CD90+Wnt3a+/CD90+). The control population had 5% Wnt3a+ fibroblasts (n=1), and in CRSwNP tissue there were 19% Wnt3a+ fibroblasts (n=3); data not shown. Further investigation is required, but the trend supports immunofluorescent quantification.

Nasal polyp derived fibroblasts decrease ciliated cells and increase epithelial permeability

Epithelial cells grown at the ALI for 21 days in co-culture with either control- or CRSwNP-hSNFs were stained for β-tubulin IV, a component of the axoneme in cilia, FOXJ1, a transcription factor used for the production of cilia, and E-cadherin, a junctional protein. Additionally, gene expression of these proteins was analyzed by qPCR for *FOXJ1* and *TUBB4B*, which is the gene for β-tubulin IV (Figure 2a–d). Monocultured hSNECs and hSNECs with control-hSNFs did not demonstrate statistically different *TUBB4B* or *FOXJ1* mRNA expression or β-tubulin IV or FOXJ1 protein by immunofluorescence. Interestingly, hSNECs co-cultured with CRSwNP-hSNFs demonstrated decreased immunofluorescence compared to control-hSNF co-culture for β-tubulin IV (0.97±0.15 vs 0.36±0.05, $p<0.01$) and FOXJ1 (68.25±3.40 vs 38.68±5.27, $p<0.01$). While a similar decrease was observed for *TUBB4B* and *FOXJ1* mRNA expression, the results were not significant.

Because the introduction of nasal polyp fibroblasts altered the epithelium, we investigated their effect on barrier function by measuring paracellular flux of apically applied FITC-dextran conjugated beads to the basolateral media of ALI cultures. While hSNEC monoculture and control-hSNF co-culture were not statistically different, co-culture with CRSwNP-hSNFs resulted in a 26% increase in epithelial permeability compared to control fibroblasts (143±9.00 vs 117±5.38, $p<0.05$) (Figure 2e).

Epithelial cells in a high Wnt milieu replicate presence of nasal polyp fibroblasts: decreased ciliated cells and elongated cell morphology

To determine if Wnt signaling alone can reduce ciliated cells in hSNEC cultures, a pharmacologic canonical Wnt agonist, CHIR99021, was used in the absence of fibroblasts. This agonist acts through inhibition of GSK3B, which dismembers the complex involved in β-catenin degradation. The resulting accumulation of β-catenin localizes to the nucleus and complexes with Lef/Tcf transcription factor leading to activation of Wnt target genes. Expression of β-catenin mRNA, *CTNNB1*, increased in epithelial cells grown with CRSwNP-hSNFs compared to untreated cultures ($p<0.05$). To compare CRSwNP-hSNFs with direct Wnt activation, we used three concentrations of CHIR99021: 1μM, 3μM, and 6μM (Figure 3e). The addition of 1μM CHIR99021 was insignificant, but the higher concentrations, 3μM and 6μM CHIR99021, showed increased *CTNNB1* mRNA ($P<0.01$ and $P<0.001$, respectively). All experiments in this study used 3μM CHIR99021.

Immunofluorescent β-tubulin IV and FOXJ1 staining showed significantly decreased ciliated cells in a high canonical Wnt environment (1.00±0.15 vs 0.27±0.05, $p<0.001$ and 80.87±3.61 vs 15.06±2.49, $p<0.001$), as well as decreased *TUBB4B* and *FOXJ1* mRNA expression compared to untreated hSNECs (1.00±0.27 vs 0.21±0.03, $p<0.05$ and 1.00±0.29 vs 0.29±0.10, $p<0.05$) (Figure 3a–d).

To evaluate epithelial morphology, we used a previously described method for quantification as the ratio of long axis to short axis [8]. E-cadherin, an adherens junctional protein, showed significant elongation of epithelial cell morphology in cultures treated with the Wnt agonist (3.33±0.24, $p<0.001$) that was also observed in co-cultures with CRSwNP-hSNFs (3.49±0.27, $p<0.001$), but not in co-cultures with control-hSNFs (1.67±0.05) compared to

monoculture hSNECs (1.62±0.10); only confocal images shown (Figures 3a and 5a). These results corroborate previous literature of CHIR99021 driving epithelial elongation [8], and for the first time show CRSwNP-hSNF derived epithelial elongation.

Epithelial organoids in CRSwNP-hSNF milieu demonstrate increased proliferative capacity

Monoclonal epithelial organoids were grown in monoculture, and co-culture with control- or CRSwNP-hSNFs. This model has hSNFs located in the basolateral compartment, not in direct contact with organoids in the apical compartment but sharing the same media. To quantify proliferative capacity, we calculated the colony forming efficiency (CFE), which is the number of organoids generated per cells seeded [18]. hSNECs co-cultured with either control-hSNFs or CRSwNP-hSNFs significantly increased CFE, but only the CRSwNP co-culture was similar to that of CHIR99021-treated hSNECs (Figure 4a, c). Further evidence of canonical Wnt signaling increasing CFE was provided by IWP2-treated organoids showing decreased CFE for both control- and CRSwNP-hSNFs.

The diameter of organoids provides a direct metric of cell proliferation [19, 20]. All diameter measurements of organoids were taken during the 10th day of culture. Groupings were organized into 50–150μm, 150–300μm, 300–500μm, and >500μm. Organoids smaller than 50μm were excluded. Noticeably, CRSwNP-hSNFs generated a significantly larger percentage of organoids over 300μm compared to both control-hSNFs and monoculture organoids (3.84±2.05 vs 33.60±3.34, $p<0.05$). Additionally, only the CRSwNP-hSNF co-culture generated organoids over 500μm by day 10 in culture (Figure 4b).

Ablation of canonical Wnt signaling increases ciliated cells and recovers epithelial cell morphology

To show that ablation of canonical Wnt activity in the co-culture model reverses decreased ciliated cells, IWP2, a Wnt secretion inhibitor was used. IWP2 inhibits *porcupine*, which prevents Wnt ligand secretion [21, 22]. Immunofluorescence for FOXJ1 (38.68±5.27 vs 65.61±1.32, $p<0.01$) and β-tubulin IV (0.37±0.06 vs 0.77±0.09, $p<0.01$) and qPCR for *TUBB4B (0.40*±0.14 vs 0.99±0.12, $p<0.05$) and *FOXJ1 (0.29*±0.06 vs 0.77±0.11, $p<0.01$) mRNA expression were increased in CRSwNP co-culture treated with IWP2 (Figure 5a–d). Additionally, a low Wnt environment reverses the elongated cell morphology observed in the presence of CRSwNP-hSNFs (3.49±0.27 vs 1.32±0.03, $p<0.0001$); only confocal images shown. *CTNNB1* mRNA was found to be reduced by qPCR (2.20±0.47 vs 0.62±0.12, $p<0.05$), verifying that IWP2 is reducing epithelial canonical Wnt signaling.

Discussion

While essential to the normal differentiation of ciliated airway epithelial cells, upregulated canonical Wnt signaling in CRSwNP has been proposed to result in a dysfunctional epithelial barrier. Passage of antigens or microbes through dysregulated epithelial junctions may trigger a chronic inflammatory response [23–26]. We propose that canonical Wnt signaling by fibroblasts in CRSwNP may contribute to features of nasal polyposis, including decreased ciliary proliferation and differentiation, altered epithelial cell morphology, increased epithelial permeability, and aberrant proliferation. Canonical Wnt activity has

recently been reported to be increased in nasal polyp tissue [8]. In this study, we provide in vitro evidence confirming that the Wnt pathway plays a role in the differentiation of ciliated epithelial cells, and we further identify nasal polyp fibroblasts as an endogenous cellular source of increased Wnt ligands in CRSwNP.

Fibroblasts and other mesenchymal cells are integral components of the sinonasal mucosa both structurally and immunologically. In chronic airway inflammatory diseases, epithelial cells and fibroblasts interact via secreted mediators to direct epithelial remodeling [23, 27–31]. Fibroblasts in nasal polyps produce a variety of pro-inflammatory mediators that promote Th2-biased inflammation [31, 32]. Among Th2-associated cytokines, TNF-α, IL-4, and IL-13 have been shown to increase fibroblast secretion of the chemokine eotaxin, which contributes to eosinophil infiltration [33–35]. Additionally, fibroblasts stimulated with TNF-α increase production of the chemokines CCL2 and MCP-1 that recruit macrophages, as well as production of IL-9, which stimulates nasal mucus production [32, 36]. Thus, fibroblasts are both affected by and contribute to the inflammatory milieu. In a study of fibroblasts isolated from control, CRS, and CRSwNP tissues, comparatively increased fibroblast numbers and proliferative activity were observed in nasal polyps [3, 31]. With respect to Wnt signaling, while basal and stimulated Wnt secretion has been demonstrated in primary lung fibroblasts [37], to our knowledge, modulation of Wnt ligand expression in nasal polyp fibroblasts has not been investigated [32].

Differential expression of Wnt in fibroblasts derived from nasal polyps versus healthy sinonasal tissue is an intriguing finding that potentially sheds new light on dysregulated epithelial-mesenchymal interactions in CRSwNP. The predilection toward *WNT3A* expression may indicate predominantly canonical Wnt pathway activation in CRSwNP, in agreement with previous reports evaluating Wnt expression in inferior turbinates compared to nasal polyp tissue [8, 9]. Furthermore, a high Wnt milieu generated pharmacologically or by co-culture with CRSwNP-hSNFs results in decreased ciliated epithelial cells and altered epithelial cell morphology. The effect of CRSwNP-hSNFs can be reversed pharmacologically with a canonical Wnt ligand secretion inhibitor, further implicating this pathway. In vivo, chronically excessive Wnt signaling may drive EMT, having a deleterious effect on mucociliary clearance due to the decrease in ciliated cells and potentially alterations in cell polarity and uncoordinated ciliary beating [8, 13, 38].

Inhibition of Wnt signaling by sequestration with IWP2 resulted in diminished epithelial β-catenin expression in control- and CRSwNP-hSNF co-cultures. The finding that IWP2 has a similar, insignificant, effect on control-hSNF co-cultures suggests that there are basal levels of canonical Wnt signaling in healthy fibroblasts. However, epithelial cells in the presence of CRSwNP-hSNFs have increased β-catenin compared to monoculture and control-hSNF co-culture, which again implicated a disease-specific alteration in canonical Wnt ligand regulation in CRSwNP-hSNFs, with a potential role in nasal polyp pathogenesis.

Recent evidence supports the concept that Wnt3a increases epithelial proliferation and has also been reported to play a causal role in the development of colon polyps [10, 18, 39]. To study the proliferative capacity of sinonasal basal cells, hSNECs were grown in organoid cultures. Organoids in the presence of CRSwNP-hSNFs were more numerous than

monoculture and control-hSNF co-culture that was reduced with a Wnt inhibitor, supporting proliferation driven by Wnt signaling. However, control-hSNFs also increased the CFE and diameter of organoids suggesting that there may be factors other than canonical Wnt signaling that aid organoid growth. Previous literature involving lung organoids showed differential expression of Wnt signaling from subtypes of mesenchymal cells and their role in epithelial differentiation. This study showed that canonical Wnt signaling drove alveolar differentiation and its inhibition drove a bronchiolar phenotype [18]. While respiratory epithelium does not express the complexity of cell types present in the lung, this literature is important to recognize the influential role of Wnt signaling and corroborates our evidence that elevated canonical Wnt signaling is aberrant to proximal airway development.

A limitation of the current study is the relatively small CRSwNP sample size, which may lead to overestimation of fibroblast Wnt3a expression. However, we believe that this cohort is representative of the larger CRSwNP population. Future studies will be needed to evaluate CRSwNP-hSNF Wnt production in various stages of polyposis and to correlate expression to disease severity. Additionally, alterations in Wnt signaling can only be proposed after injury and not as the initiating event, since all models had fibroblasts or Wnt modulators present during the time of differentiation. It is not possible to determine from the present study whether these changes would also occur if introduced to fully differentiated ALI cultures. That being said, previous reports indicate that Wnt activation is downstream in polyp pathogenesis, since introduction of Wnt agonist to a fully differentiated ALI culture did not induce morphological changes observed during differentiation [8]. Although independent Wnt signaling activation is not sufficient to initiate pathology in intact airway epithelia, it may sustain tissue remodeling observed after injury to the nasal epithelium.

Conclusion

Fibroblasts derived from nasal polyps decrease ciliation, elongate cell morphology, increase epithelial permeability, and increase the proliferative capacity of basal cells, distinct from co-culture with control sinonasal fibroblasts. We propose that these effects are mediated by increased canonical Wnt signaling in CRSwNP fibroblasts, which have significantly greater expression of *WNT3A* relative to control-hSNFs and are found in greater abundance in CRSwNP tissue. Furthermore, inhibition of canonical Wnt signaling rescues the altered epithelial cell characteristics induced by polyp fibroblast co-culture. These results suggest that abnormal interactions between epithelial cells and fibroblasts are a feature of nasal polyposis and supports the concept that dysregulated Wnt signaling contributes to impairment of epithelial function in CRSwNP.

Acknowledgments

Funding: National Institutes of Health: R01AI072502 (A.P.L.)

References

1. Stevens WW, Schleimer RP, Kern RC. Chronic Rhinosinusitis with Nasal Polyps. J Allergy Clin Immunol Pract. 2016; 4(4):565–72. [PubMed: 27393770]

2. Van Crombruggen K, et al. Pathogenesis of chronic rhinosinusitis: inflammation. J Allergy Clin Immunol. 2011; 128(4):728–32. [PubMed: 21868076]
3. Carroll WW, et al. Vitamin D deficiency is associated with increased human sinonasal fibroblast proliferation in chronic rhinosinusitis with nasal polyps. Int Forum Allergy Rhinol. 2016; 6(6):605–10. [PubMed: 26750566]
4. Czerny MS, et al. Histopathological and clinical analysis of chronic rhinosinusitis by subtype. Int Forum Allergy Rhinol. 2014; 4(6):463–9. [PubMed: 24574266]
5. Orlandi RR, et al. International Consensus Statement on Allergy and Rhinology: Rhinosinusitis. Int Forum Allergy Rhinol. 2016; 6(Suppl 1):S22–209. [PubMed: 26889651]
6. Lane AP. The role of innate immunity in the pathogenesis of chronic rhinosinusitis. Curr Allergy Asthma Rep. 2009; 9(3):205–12. [PubMed: 19348720]
7. Vladar EK, et al. Airway epithelial homeostasis and planar cell polarity signaling depend on multiciliated cell differentiation. JCI Insight. 2016; 1(13)
8. Boscke R, et al. Wnt Signaling in Chronic Rhinosinusitis with Nasal Polyps. Am J Respir Cell Mol Biol. 2017; 56(5):575–584. [PubMed: 28059551]
9. Schmid A, et al. Modulation of Wnt signaling is essential for the differentiation of ciliated epithelial cells in human airways. FEBS Lett. 2017; 591(21):3493–3506. [PubMed: 28921507]
10. Vincan E, et al. The Central Role of Wnt Signaling and Organoid Technology in Personalizing Anticancer Therapy. Prog Mol Biol Transl Sci. 2018; 153:299–319. [PubMed: 29389521]
11. Baarsma HA, et al. Activation of WNT/beta-catenin signaling in pulmonary fibroblasts by TGF-beta(1) is increased in chronic obstructive pulmonary disease. PLoS One. 2011; 6(9):e25450. [PubMed: 21980461]
12. Valenta T, et al. Wnt Ligands Secreted by Subepithelial Mesenchymal Cells Are Essential for the Survival of Intestinal Stem Cells and Gut Homeostasis. Cell Rep. 2016; 15(5):911–918. [PubMed: 27117411]
13. Ghahhari NM, Babashah S. Interplay between microRNAs and WNT/beta-catenin signalling pathway regulates epithelial-mesenchymal transition in cancer. Eur J Cancer. 2015; 51(12):1638–49. [PubMed: 26025765]
14. Wang X, et al. Feedback Activation of Basic Fibroblast Growth Factor Signaling via the Wnt/beta-Catenin Pathway in Skin Fibroblasts. Front Pharmacol. 2017; 8:32. [PubMed: 28217097]
15. Hackett NR, et al. The human airway epithelial basal cell transcriptome. PLoS One. 2011; 6(5):e18378. [PubMed: 21572528]
16. Ramanathan M Jr, Lane AP. A comparison of experimental methods in molecular chronic rhinosinusitis research. Am J Rhinol. 2007; 21(3):373–7. [PubMed: 17621826]
17. Sussan TE, et al. Nrf2 reduces allergic asthma in mice through enhanced airway epithelial cytoprotective function. Am J Physiol Lung Cell Mol Physiol. 2015; 309(1):L27–36. [PubMed: 25957295]
18. Lee JH, et al. Anatomically and Functionally Distinct Lung Mesenchymal Populations Marked by Lgr5 and Lgr6. Cell. 2017; 170(6):1149–1163e12. [PubMed: 28886383]
19. Zacharias WJ, et al. Regeneration of the lung alveolus by an evolutionarily conserved epithelial progenitor. Nature. 2018; 555(7695):251–255. [PubMed: 29489752]
20. Chung MI, et al. Niche-mediated BMP/SMAD signaling regulates lung alveolar stem cell proliferation and differentiation. Development. 2018; 145(9)
21. Du Y, et al. Regulation of metastasis of bladder cancer cells through the WNT signaling pathway. Tumour Biol. 2015; 36(11):8839–44. [PubMed: 26069102]
22. Moon J, et al. Blockade to pathological remodeling of infarcted heart tissue using a porcupine antagonist. Proc Natl Acad Sci U S A. 2017; 114(7):1649–1654. [PubMed: 28143939]
23. Meng J, et al. The development of nasal polyp disease involves early nasal mucosal inflammation and remodelling. PLoS One. 2013; 8(12):e82373. [PubMed: 24340021]
24. Hupin C, et al. Features of mesenchymal transition in the airway epithelium from chronic rhinosinusitis. Allergy. 2014; 69(11):1540–9. [PubMed: 25104359]

25. Soyka MB, et al. Defective epithelial barrier in chronic rhinosinusitis: the regulation of tight junctions by IFN-gamma and IL-4. J Allergy Clin Immunol. 2012; 130(5):1087–1096e10. [PubMed: 22840853]
26. Schleimer RP. Immunopathogenesis of Chronic Rhinosinusitis and Nasal Polyposis. Annu Rev Pathol. 2017; 12:331–357. [PubMed: 27959637]
27. Knight D. Epithelium-fibroblast interactions in response to airway inflammation. Immunol Cell Biol. 2001; 79(2):160–4. [PubMed: 11264711]
28. Al-Muhsen S, Johnson JR, Hamid Q. Remodeling in asthma. J Allergy Clin Immunol. 2011; 128(3):451–62. quiz 463–4. [PubMed: 21636119]
29. Van Bruaene N, Bachert C. Tissue remodeling in chronic rhinosinusitis. Curr Opin Allergy Clin Immunol. 2011; 11(1):8–11. [PubMed: 21150430]
30. Boulet LP. Airway remodeling in asthma: update on mechanisms and therapeutic approaches. Curr Opin Pulm Med. 2018; 24(1):56–62. [PubMed: 29076828]
31. Carroll WW, et al. Fibroblast levels are increased in chronic rhinosinusitis with nasal polyps and are associated with worse subjective disease severity. Int Forum Allergy Rhinol. 2016; 6(2):162–8. [PubMed: 26370180]
32. Homma H, et al. Multiplex analyses of cytokine and chemokine release from the cultured fibroblast of nasal polyps: the effect of IL-17A. Acta Otolaryngol. 2013; 133(10):1065–72. [PubMed: 24032570]
33. Yoshifuku K, et al. IL-4 and TNF-alpha increased the secretion of eotaxin from cultured fibroblasts of nasal polyps with eosinophil infiltration. Rhinology. 2007; 45(3):235–41. [PubMed: 17956026]
34. Oyer SL, et al. Cytokine correlation between sinus tissue and nasal secretions among chronic rhinosinusitis and controls. Laryngoscope. 2013; 123(12):E72–8. [PubMed: 23852962]
35. Fukuda K, Nishida T, Fukushima A. Synergistic induction of eotaxin and VCAM-1 expression in human corneal fibroblasts by staphylococcal peptidoglycan and either IL-4 or IL-13. Allergol Int. 2011; 60(3):355–63. [PubMed: 21502805]
36. Kouzaki H, et al. Role of platelet-derived growth factor in airway remodeling in rhinosinusitis. Am J Rhinol Allergy. 2009; 23(3):273–80. [PubMed: 19490801]
37. Aumiller V, et al. WNT/beta-catenin signaling induces IL-1beta expression by alveolar epithelial cells in pulmonary fibrosis. Am J Respir Cell Mol Biol. 2013; 49(1):96–104. [PubMed: 23526221]
38. Tilley AE, et al. Cilia dysfunction in lung disease. Annu Rev Physiol. 2015; 77:379–406. [PubMed: 25386990]
39. Takahashi Y, et al. A Refined Culture System for Human Induced Pluripotent Stem Cell-Derived Intestinal Epithelial Organoids. Stem Cell Reports. 2018; 10(1):314–328. [PubMed: 29233552]

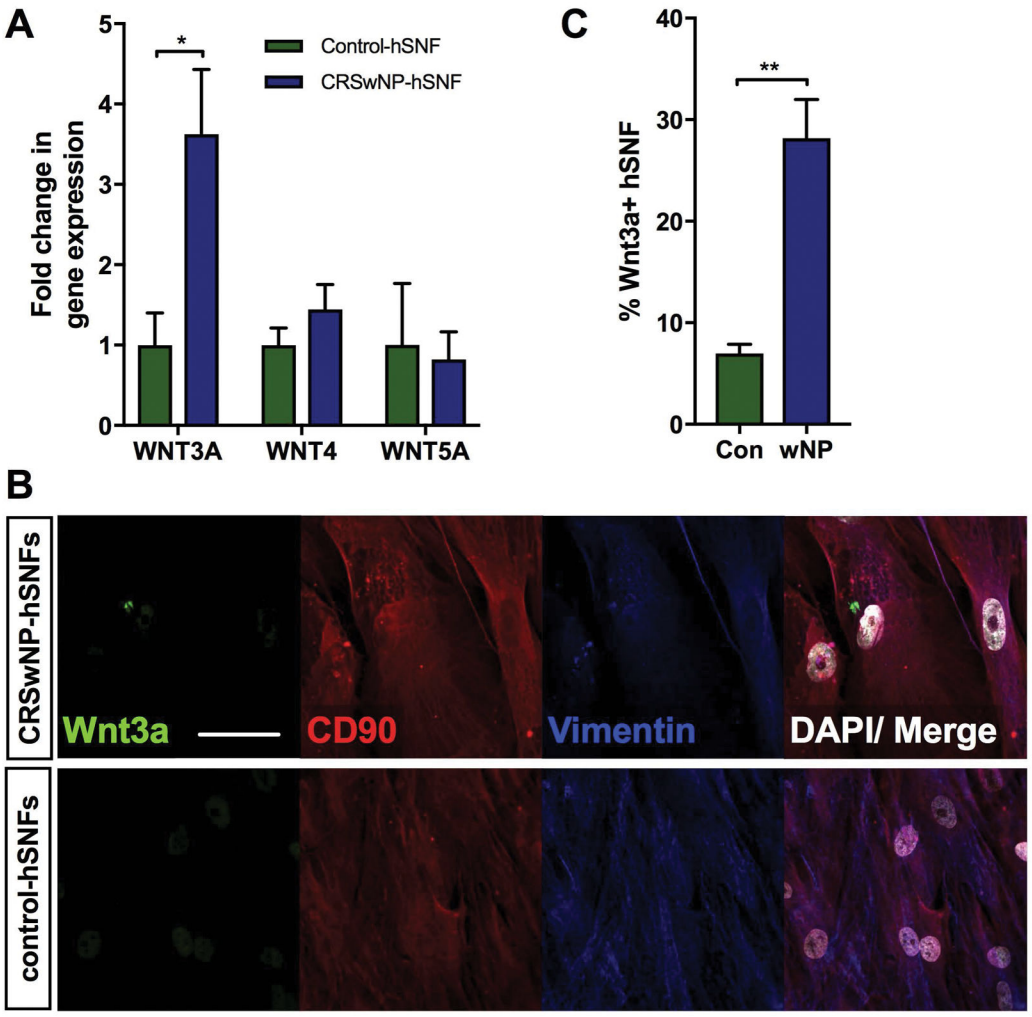

Figure 1.

Nasal polyp derived fibroblasts have elevated canonical *WNT3A* mRNA expression. (A) mRNA expression of *WNT3a*, *WNT4*, and *WNT5a* in CRSwNP-hSNF relative to control-hSNFs. (B) Confocal image showing Wnt3a hSNFs: Wnt3a (green), CD90 (red), vimentin (blue), DAPI (white). (C) Percent Wnt3a+ hSNFs. 40x magnification. Scale bar: 50μm. Data is presented as mean±SEM. *p<0.05, **p<0.01

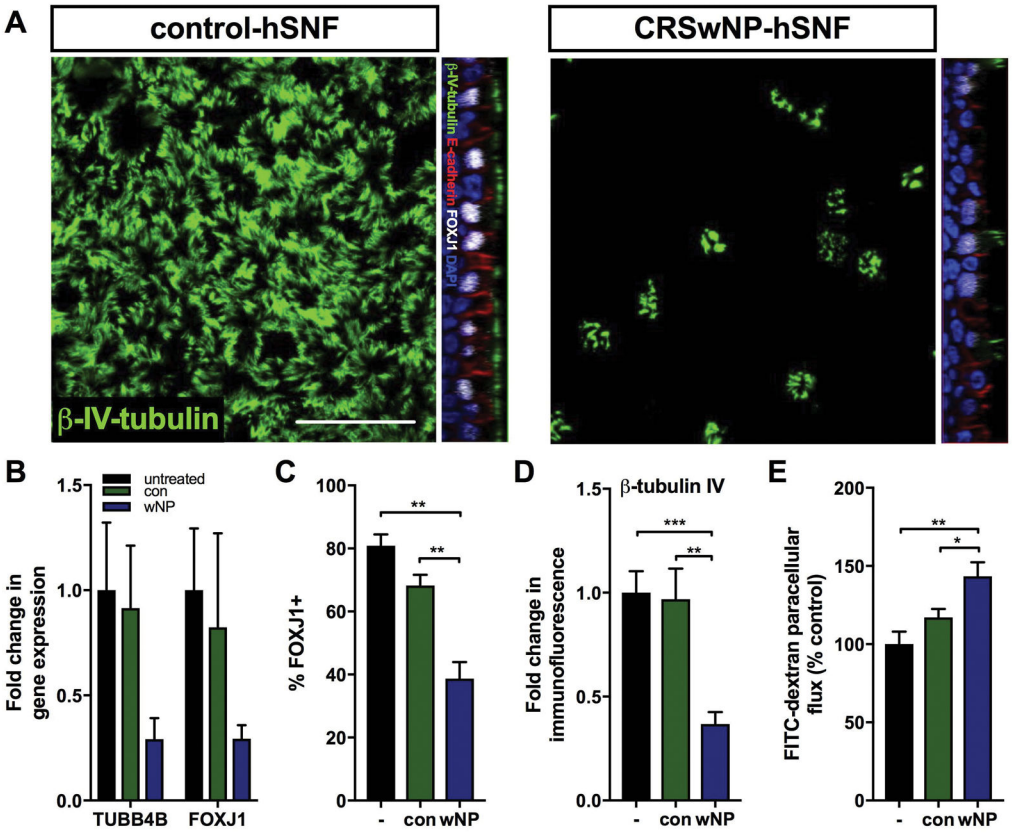

Figure 2.

Nasal polyp derived fibroblasts decrease ciliated epithelial cells and increase epithelial permeability. (A) Top-down: Epithelial β-tubulin IV immunofluorescence for hSNECs + Control-hSNFs and hSNECs + CRSwNP-hSNFs. Orthogonal image: B-tubulin IV (green), E-cadherin (red), FOXJ1 (white), DAPI (blue) (B) Expression of *TUBB4B* and *FOXJ1* mRNA relative to monoculture hSNECs. (C) Percentage of FOXJ1+ cells calculated by immunofluorescence. (D) β-tubulin IV immunofluorescence intensity relative to monoculture hSNECs Mean Gray Value. (E) Transepithelial permeability assessed by FITC-dextran flux. For B–E: hSNECs (−), hSNECs + Control-hSNFs (con), hSNECs + CRSwNP-hSNFs (wNP). All images use 40x magnification. Scale bar: 50μm. Data is presented as mean±SEM. *p<0.05, **p<0.01, ***p<0.001

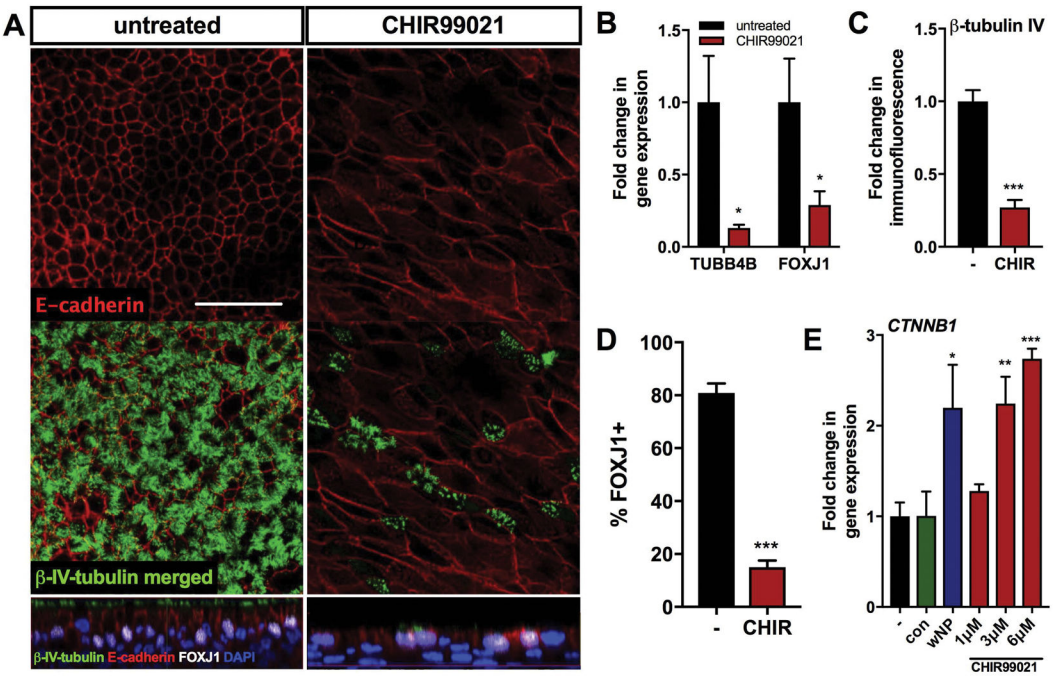

Figure 3.

Epithelial cells in a high Wnt milieu replicate decreased ciliary differentiation and elongated cell morphology. (A) Confocal images of untreated hSNECs and hSNECs treated with 3μM CHIR99021 stained for β-tubulin IV (green), E-cadherin (red), FOXJ1 (white), DAPI (blue). (B) mRNA expression of *TUBB4B* and *FOXJ1* CHIR99021-treated hSNECs relative to untreated hSNECs (−). (C) Quantified immunofluorescence of β-tubulin IV CHIR99021-treated hSNECs relative to untreated hSNECs (−) Mean Gray Value. (D) Percentage of FOXJ1+ cells calculated by immunofluorescence. (E) mRNA expression of *CTNNB1* for hSNECs with control-hSNFs (con), CRSwNP-hSNFs (wNP), and CHIR99021-treated hSNECs (1μM, 3μM, 6μM) relative to untreated hSNECs (−). All images use 40x magnification. Scale bar: 50μm. Data is presented as mean±SEM. *p<0.05, **p<0.01, ***p<0.001

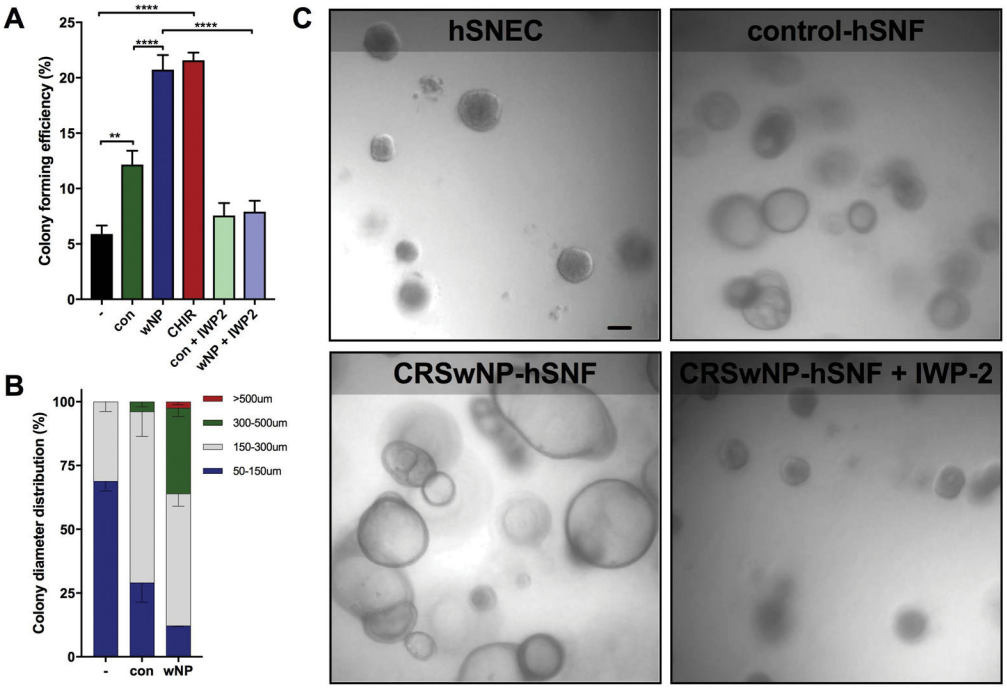

Figure 4.

Epithelial organoids in CRSwNP-hSNF milieu demonstrate increased proliferation. (A) Colony forming efficiency calculated as percentage of organoids per cells plated. (B) Distribution percentage of organoids by diameter. (C) PMT images of organoids at 6x magnification using a Zeiss 780 confocal microscope. Scale bar: 50μm. Data is presented as mean±SEM. *P<0.05, **p<0.01, ****p<0.0001

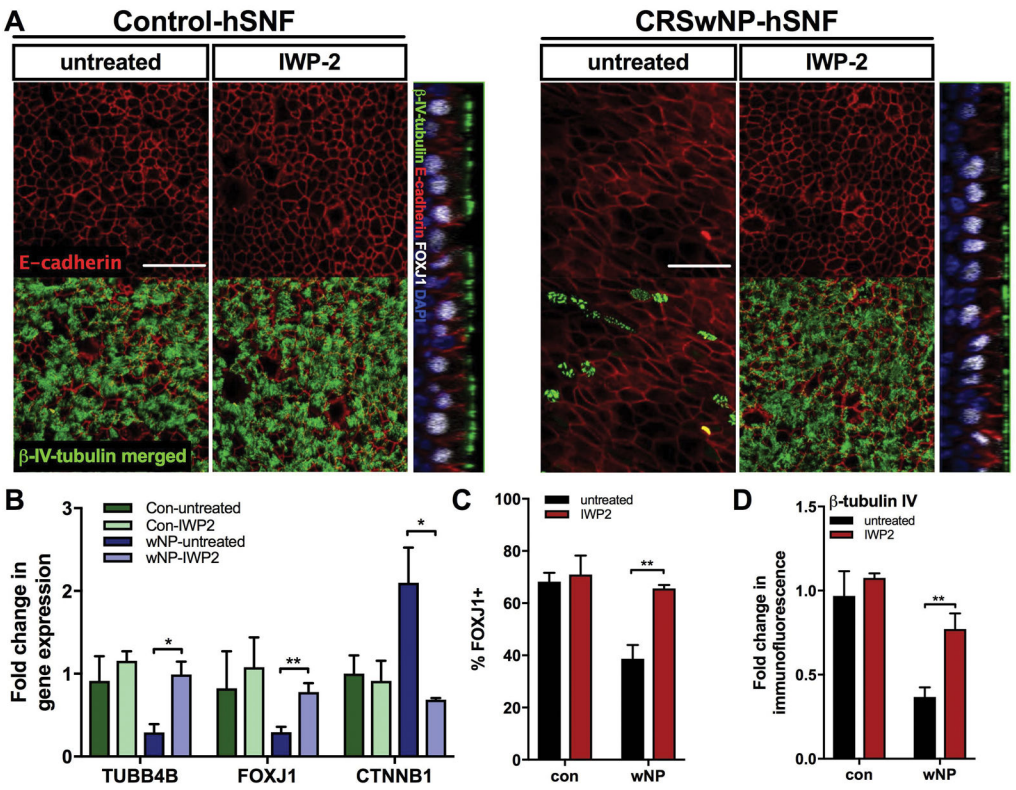

Figure 5.

Ablation of canonical Wnt signaling increases ciliary differentiation and ameliorates cell morphology. hSNEC co-culture with control- or CRSwNP-hSNFs were either untreated or treated with 2.5μM IWP2. (A) Confocal images of β-tubulin IV (green), E-cadherin (red), FOXJ1 (white), and DAPI (blue). (B) mRNA expression of *TUBB4B*, *FOXJ1*, and *CTNNB1* relative to monoculture hSNECs. (C) Percentage of FOXJ1+ cells calculated by immunofluorescence. (D) Quantified immunofluorescence of β-tubulin IV relative to monoculture hSNECs Mean Gray Value. All images use 40x magnification. Scale bar: 50μm. Data is presented as mean±SEM. *p<0.05, **p<0.01

Table 1

Human subjects. Thirty-four human subjects (25 controls and 9 CRSwNP) were enrolled in this study.

	Control	CRSwNP
Subjects	25	9
Age (yrs)	50 ± 15	53 ± 16
Sex		
male	9	3
female	16	6